NANOSYSTEMS:
PHYSICS, CHEMISTRY, MATHEMATICS

Original article

Chebanenko M.I., et al. *Nanosystems: Phys. Chem. Math.*, 2023, **14** (6), 705–712.
http://nanojournal.ifmo.ru
DOI 10.17586/2220-8054-2023-14-6-705-712

Planetary grinding's impact on the structure and photocatalytic characteristics of urea-derived g-C_3N_4 nanocrystals

Maria I. Chebanenko[1], Lev A. Lebedev[1], Maksim I. Tenevich[1], Ekaterina Yu. Stovpiaga[1], Vadim I. Popkov[1]

[1]Ioffe Institute, St. Petersburg, Russia

Corresponding author: Maria I. Chebanenko, m_chebanenko@list.ru

PACS 61.43.Gt, 61.46.+w

ABSTRACT The burgeoning interest in two-dimensional materials derived from graphite carbon nitride (g-C_3N_4) stems from its non-toxicity, exceptional charge carrier mobility, and UV-vis absorption capabilities. Crucially, g-C_3N_4's performance hinges on its specific surface area. We investigate how planetary grinding impacts the crystal and electronic structures of g-C_3N_4 nanocrystals. Six samples, subjected to varying durations of mechanical treatment, underwent comprehensive characterization using a complex of physico-chemical methods. Notably, planetary grinding substantially increases the specific surface area of g-C_3N_4 nanocrystals while preserving their electronic structure. Furthermore, we assessed the photocatalytic performance of these samples in decomposing antibiotics under visible light. The nanocrystalline powder with an enhanced specific surface area demonstrated a remarkable efficiency in tetracycline hydrochloride decomposition. In summary, our study highlights the potential of planetary grinding as a means to augment g-C_3N_4's specific surface area, positioning it as a promising platform for the development of contemporary, eco-friendly photocatalysts.

KEYWORDS g-C_3N_4, graphitic carbon nitride, two-dimensional structures, mechanical processing, photocatalysis

ACKNOWLEDGEMENTS This work was supported by the Russian Science Foundation (project No. 23-23-00328).

FOR CITATION Chebanenko M.I., Lebedev L.A., Tenevich M.I., Stovpiaga E.Yu., Popkov V.I. Planetary grinding's impact on the structure and photocatalytic characteristics of urea-derived g-C_3N_4 nanocrystals. *Nanosystems: Phys. Chem. Math.*, 2023, **14** (6), 705–712.

1. Introduction

The rapid expansion of the pharmaceutical industry, characterized by the continuous development and large-scale production of medicinal products, has brought about a pressing need for the safe disposal of industrial wastewater [1–4]. Presently, the photocatalytic oxidation of pharmaceutical compounds under solar irradiation has emerged as a promising and eco-friendly method for treating wastewater generated during pharmaceutical manufacturing processes [5–8]. This technique harnesses the synergistic interplay of a photocatalyst and visible light. By absorbing photons, the photocatalyst generates electron-hole pairs, which actively engage in subsequent reactions. These reactions culminate in the production of potent oxidizing agents that effectively degrade organic contaminants.

Many established photocatalysts primarily function within the ultraviolet domain of the electromagnetic spectrum are often composed of costly elements [9–11]. Consequently, the scientific community has turned its attention to graphitic carbon nitride (g-C_3N_4) in recent years. g-C_3N_4 stands out as a semiconductor material comprised of readily available chemical components, exhibiting remarkable chemical stability and the capacity to absorb visible light [7, 10, 12]. However, the photocatalytic performance of this material is constrained by its relatively modest specific surface area and a propensity for rapid charge carrier recombination [2].

To address this limitation, researchers have explored various strategies for exfoliating bulk graphitic carbon nitride into nanosheets. This exfoliation process enhances both the specific surface area and the number of active sites on g-C_3N_4, thereby reducing volumetric charge carrier recombination [13]. For example, a study outlined in [14] introduces a thermal exfoliation method conducted at 550 °C for 1 – 3 hours, resulting in an increased specific surface area and improved photocatalytic capabilities for NO removal under visible light. Research detailed in [15] describes the successful exfoliation of g-C_3N_4 using sulfuric acid for 8 hours, followed by ultrasonic treatment, rendering the material suitable for use as a photocatalyst in hydrogen evolution reactions. An effective approach to ultrasonic exfoliation of g-C_3N_4 is proposed in [16], where bulk g-C_3N_4 powder, dispersed in a N-Methyl pyrrolidone (NMP) solution, is subjected to ultrasonic treatment, yielding nanosheets suitable for photocatalytic hydrogen production. Additionally, article [12] highlights the beneficial impact of steam exfoliation on the electrochemical properties of g-C_3N_4. Nevertheless, all these

methods are characterized by their complex and time-consuming procedures, reliance on expensive chemical reagents, and the need for specialized equipment.

The present study introduces a promising approach to exfoliate bulk graphitic carbon nitride utilizing mechanical forces in a planetary mill. The investigation shows the influence of the duration of mechanical treatment on the crystalline and electronic structure of the resultant g-C_3N_4. Notably, it is revealed that the mechanical grinding exerts a positive impact on the specific surface area. The study culminates in a photocatalytic assessment involving the oxidation of tetracycline hydrochloride under visible light. The research findings strongly suggest that exfoliation via a planetary mill holds significant potential for enhancing the photocatalytic activity of graphitic carbon nitride. This, in turn, opens up promising avenues for the utilization of such materials as the foundation for catalysts employed in the neutralization of hazardous compounds present in pharmaceutical wastewater.

2. Materials and methods

2.1. Materials

Urea (99.8 %, CH_4N_2O) was purchased from NevaReaktiv. Tetracycline hydrochloride (95 %, $C_{22}H_{24}N_2O_8{\cdot}HCl$) was obtained from neoFroxx. All the reagents used in this research work are analytical grade. Deionized water was obtained from the analytical laboratory.

2.2. Synthesis of g-C_3N_4 nanopowder

To obtain graphitic carbon nitride, urea powder was placed in a quartz crucible. Thermal polymerization was conducted for 1 hour at a temperature of 550 °C in an ambient air atmosphere. The yield of the target product when using urea as a precursor was 2 % by mass [17, 18].

The resulting powder was divided into 6 portions for subsequent grinding. 1 gram of the sample, along with 10 mL of ethanol and 7 agate balls, were loaded into a 30 mL capacity ball mill jar. The duration of mechanical treatment varied from 30 to 150 minutes, and the milling was performed at a drum rotation speed of 300 revolutions per minute. The obtained suspensions were dried at 100 °C until complete removal of ethanol. As a result, a series of six samples was obtained, differing in the duration of planetary milling (CN-0, CN-30, CN-60, CN-90, CN-120, and CN-150).

2.3. Physico-chemical characterization

Structural changes of the g-C_3N_4 sample during grinding were recorded by Shimadzu XRD-6000 X-ray diffractometer equipped (CuKα radiation, $\lambda = 0.154051$ nm) in the range 5 – 80° (2θ) with a scanning step of 0.01° and integration time for each point 1 s. The average size of the crystallites was estimated using Debye–Scherrer's equation [19]:

$$D = \frac{0.94 \cdot \lambda}{\beta \cdot \cos\theta},$$

where λ is the wavelength of the incident radiation (CuK$\alpha = 0.154$ nm); β is the full width at half maximum in radians; θ is the Bragg angle in radians [19].

The degree of crystallinity of the samples was calculated based on the analysis of X-ray diffraction pattern profile:

$$\text{Crystallinity degree } = \frac{\text{Area of all the crystalline peaks}}{\text{Area of all the crystalline and amorpous peaks}}.$$

The nanopowder morphology was examined through scanning electron microscopy (SEM) using a Tescan Vega 3 SBH scanning electron microscope.

N_2 adsorption-desorption measurements were conducted with an 3FLEX Surface Area and Porosity Analyzer at a standard mode, at a temperature of 77 K. The specific surface area was calculated using the Brunauer–Emmett–Teller (BET) method. Pore size distribution plots were generated from the desorption branch of the isotherm using the Barrett–Joyner–Halenda (BJH) method.

Diffuse reflection spectra were acquired at room temperature within the 350 – 700 nm range using an Avaspec-ULS2048CL-EVO spectrometer equipped with an AvaSphere-30-REFL refractometric integration sphere. The obtained diffuse reflection spectra were analyzed using the Kubelka–Munk function [7, 20]:

$$F(R) = \frac{(1-R)^2}{2R},$$

where R represents the diffuse reflection of the sample.

To determine the values of the optical bandgap, the Tauc plot was utilized:

$$h\upsilon \cdot F(R)^{1/n} = A(h\upsilon - E_g),$$

where A is the proportionality coefficient, n is the power index indicating the nature of the transition, $h\upsilon$ is the photon energy, and E_g is the optical bandgap.

2.4. Photocatalytic measurements

Tetracycline hydrochloride (TCHCl) was selected as the model antibiotic, with an initial solution concentration of 0.03 g/L. A 1 mg quantity of catalyst powder was thoroughly dispersed in the initial antibiotic solution and placed within a 10 mL capacity photocatalytic reactor cuvette. The solution was then stirred in the dark for 1 hour to establish an adsorption-desorption equilibrium.

Subsequently, the solution was exposed to LEDs with a power consumption of 24 W and a peak wavelength of 405 nm, while being continuously stirred under visible radiation. In-situ measurements were conducted using an Avaspec-ULS2048CL-EVO spectrometer equipped with an Avalight-XE Pulsed Xenon Lamp.

The degree of antibiotic decomposition under the influence of visible radiation in the presence of the catalyst was determined using the following formula:

$$\text{Rem. Eff.} = \frac{(C_0 - C)}{C_0} \cdot 100\ \%,$$

where C_0 represents the initial concentration of the TCHCl solution, and C is the concentration of the TCHCl solution after exposure to light.

3. Results and discussion

3.1. Powder X-ray diffraction

The crystalline structure and phase purity of the prepared series of samples were confirmed through X-ray phase analysis. Fig. 1(a) illustrates diffraction patterns for the initial CN-0 sample and samples subjected to mechanical grinding with varying durations (CN-30, CN-60, CN-90, CN-120, and CN-150). All obtained graphs exhibit a typical pattern for graphitic carbon nitride.

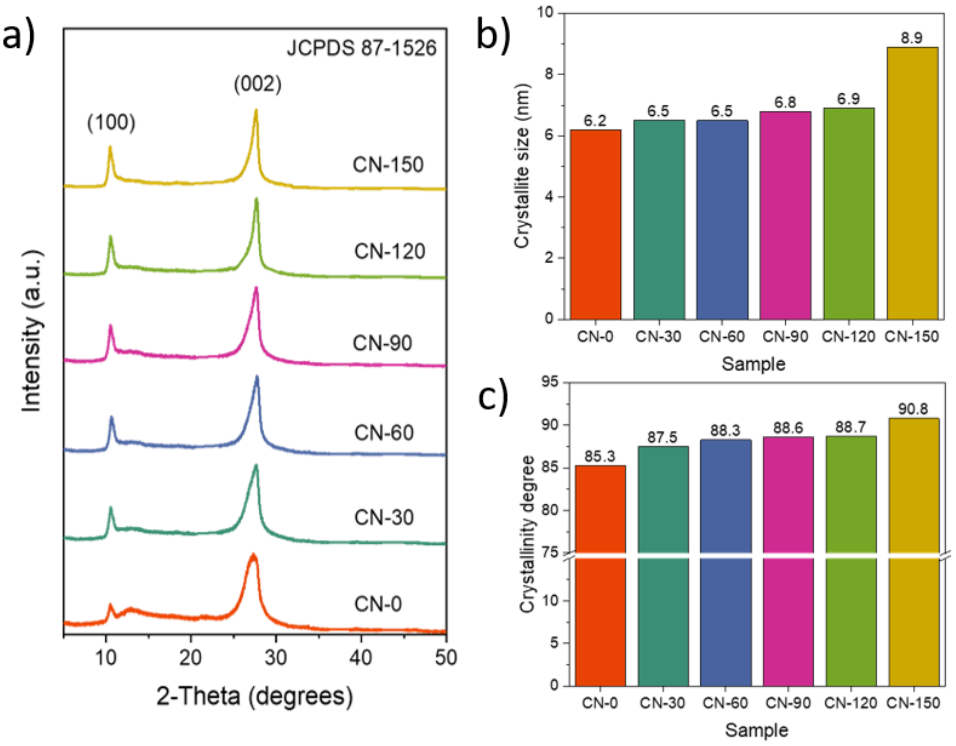

FIG. 1. (a) Powder X-ray diffraction patterns; (b) crystallinity degree and (c) crystallite size of CN-0, CN-30, CN-60, CN-90, CN-120 and CN-150 samples

The X-ray diffraction patterns display two prominent reflections at approximately 13° and 27°, corresponding to the diffraction planes (100) and (002), respectively (JCPDS card 87-1526) [21, 22].

The concurrent increase in X-ray reflection intensity and reduction in their width as grinding time increases may indicate an expansion of the coherent scattering domain. The average crystallite size, determined along the crystallographic direction (002), is presented in Fig. 1(b) as a bar chart.

Considering that nanocrystalline graphitic carbon nitride comprises a plethora of irregularly shaped and randomly oriented flakes, it is posited that mechanical treatment induces the ordering and straightening of the edges of individual nanosheets. This phenomenon suggests a transition towards a more planar configuration, as supported by the heightened degree of crystallinity observed in the samples (Fig. 1(c)).

3.2. Scanning electron microscopy

The alterations in the morphology of graphitic carbon nitride due to the impact of planetary milling were documented using scanning electron microscopy (SEM). In Fig. 2(a), the original graphitic carbon nitride powder is depicted as consisting of randomly oriented two-dimensional sheets with irregular edges. Mechanical treatment induces a transformation in the shape of these sheets, accompanied by their partial agglomeration.

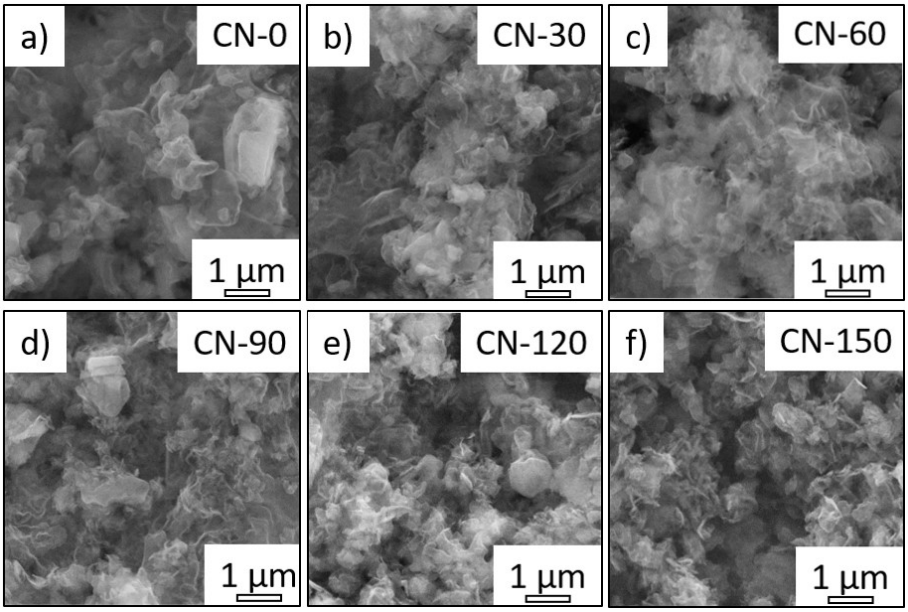

FIG. 2. SEM images of (a) CN-0; (b)CN-30; (c) CN-60; (d) CN-90; (e) CN-120 and (f) CN-150 nanopowders

3.3. N_2 adsorption-desorption analysis

The textural characteristics of the CN-0, CN-30, CN-60, CN-60, CN-90, CN-120, and CN-150 samples were investigated using the low-temperature nitrogen adsorption-desorption method. The resulting isotherms, as depicted in Fig. 3(a), are classified as Type IV, indicating the mesoporous nature of this material. Notably, the hysteresis loops displayed pronounced features associated with the capillary condensation of gas within the mesopores. This behavior is indicative of mesoporous structures.

Further analysis, as shown in Fig. 3(b), through pore size distribution plotting, confirms the presence of pores with diameters falling within the range of 2 – 50 nm. It is noteworthy that the porosity of the samples experiences a marginal increase during the planetary milling process, primarily attributed to the creation of additional interlayer space within the graphitic carbon nitride material, as evidenced in Fig. 3(c).

The specific surface area was determined using the linear form of the BET equation, and the resulting specific surface area values are illustrated in Fig. 3(c). It is evident that consecutive increases in specific surface area values occur during the grinding process in the planetary mill.

Graphitic carbon nitride is characterized by a layered structure comprising tri-s-triazine units, as depicted in Fig. 4 [23]. These layers in g-C_3N_4 are weakly bonded together by van der Waals forces, facilitating easy exfoliation and, consequently, an increase in the available surface area for sorption. It is postulated that the sequential rise in specific surface area values is achieved by reducing the stack thickness (h) during mechanical treatment. Prolonged mixing in the planetary mill leads to partial particle agglomeration, resulting in a further decrease in specific surface area and an increase in stack thickness.

3.4. Diffuse reflectance spectroscopy

The optical properties of the sample series were investigated through diffuse reflectance spectroscopy. In Fig. 5(a), absorption spectra within the UV-visible range are presented for the CN-0, CN-30, CN-60, CN-90, CN-120, and CN-150 samples. The results reveal that the grinding process in the planetary mill leads to a shift in the absorption edge towards the visible spectrum ($\lambda \geq 400$ nm). This observed "redshift" effect signifies an enhanced light absorption capability of graphitic carbon nitride within the visible portion of the spectrum, resulting in an increased generation of electron-hole pairs.

To determine the optical bandgap width for the samples, Tauc plots were constructed. Fig. 5(b) illustrates the spectral dependencies $[R(F)h\nu]^{1/2}$ derived from the obtained spectral absorption coefficient data. The bandgap width values were obtained through extrapolation of the linear region of the spectrum to the abscissa axis. As anticipated, there were

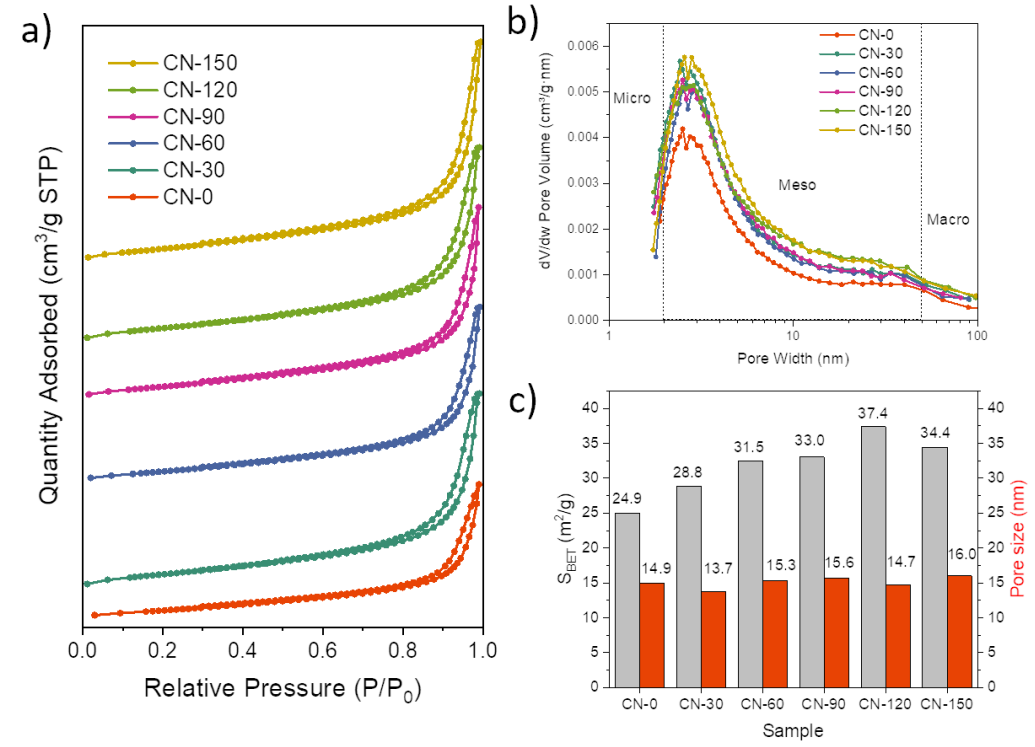

FIG. 3. (a) Nitrogen adsorption-desorption isotherms; (b) the pore size distribution results calculated from the BJH desorption pore volume data; (c) BET surface area and pore size of CN-0, CN-30, CN-60, CN-90, CN-120 and CN-150 samples

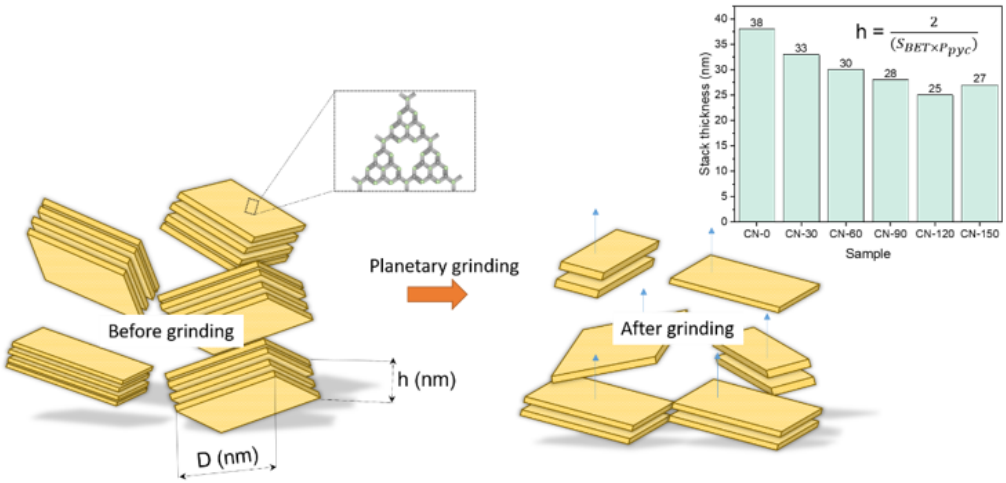

FIG. 4. Schematic representation of the mechanical grinding process

no substantial alterations in the electronic structure after mechanical grinding. The optical bandgap width for the sample series exhibited variations within the range of 3.84 – 3.85 eV.

3.5. Photocatalytic test

The influence of mechanical grinding on the photocatalytic performance of graphitic carbon nitride was evaluated during the oxidation of tetracycline hydrochloride under visible light ($\lambda = 405$ nm). The photocatalytic experiment was preceded by a dark control test. Solutions containing specified quantities of CN-0, CN-30, CN-60, CN-90, CN-120, and CN-150 powders were agitated in darkness for 15 minutes to establish an adsorption equilibrium. Additionally, a control solution of tetracycline hydrochloride was exposed to visible light to rule out the possibility of its spontaneous degradation under illumination. Fig. 6(a) illustrates the representative absorption spectra of tetracycline hydrochloride recorded over a 60-minute duration in the presence of the CN-150 sample. Fig. 6(b) depicts the concentration ratios

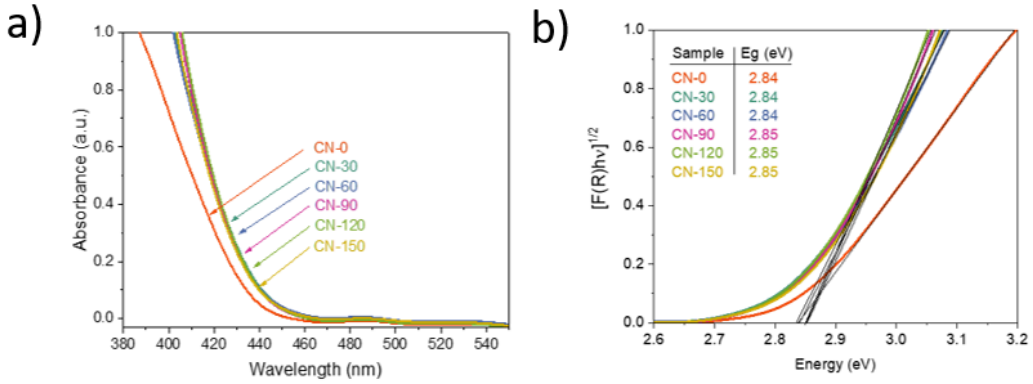

FIG. 5. (a) UV-vis diffuse reflectance spectroscopy; (b) Tauc plots of CN-0, CN-30, CN-60, CN-90, CN-120 and CN-150 samples

(C/C_0). It is evident that the duration of mechanical treatment on the nanocrystalline graphitic carbon nitride powder exerts a favorable influence on its photocatalytic activity.

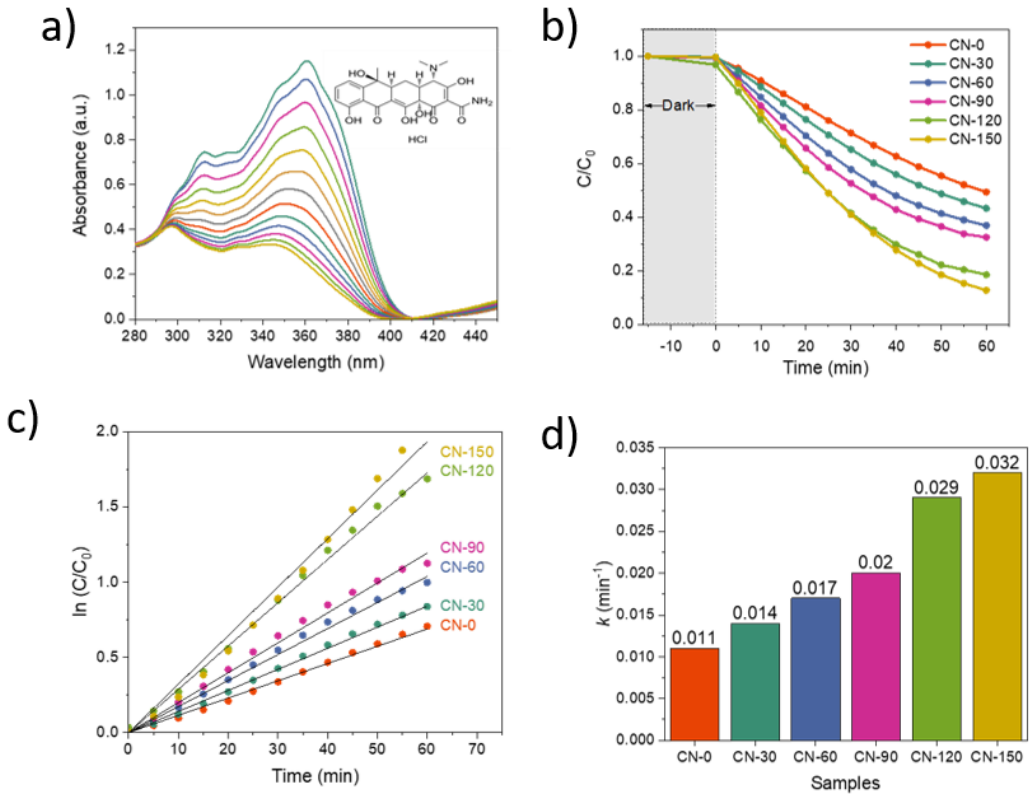

FIG. 6. (a) The decomposition spectrum of tetracycline hydrochloride in the presence of CN-150; (b) photocatalytic degradation curves of TCHCl; (c) pseudo-first-order kinetic curves of the samples; (d) the calculated kinetic constants

To quantitatively assess the catalytic activity, the apparent first-order rate constant was determined by plotting the natural logarithm of (C/C_0) against the duration of the photocatalytic experiment. The resulting values are presented as a bar chart in Fig. 6(d). It was ascertained that this exfoliation method engenders a threefold enhancement in the photocatalytic capabilities of the material.

The findings affirm a consistent augmentation in photocatalytic activity with prolonged mechanical exfoliation time. It is notable that the most significant increase in photocatalytic activity is observed for the CN-120 sample, characterized by the highest specific surface area and the thinnest stack thickness of graphitic carbon nitride. It is postulated that further extension of the mechanical treatment may lead to a gradual reduction in photocatalytic activity due to the re-agglomeration of g-C_3N_4 nanolayers.

4. Conclusions

The original nanocrystalline powder of graphitic carbon nitride was synthesized via the thermal polymerization of urea at 550 °C in an ambient air atmosphere. Subsequently, the resulting calcined powder underwent mechanical grinding in a planetary mill for various durations, ranging from 0 to 150 minutes. This extended mechanical treatment led to a notable improvement in the powder's crystallinity, concomitant with the straightening and ordering of the nanosheets comprising the graphitic carbon nitride. Notably, there was an expansion in the coherent scattering domain as the synthesis temperature increased. Remarkably, the electronic structure of the powder remained largely unaltered, with the bandgap width consistently hovering around 2.8 eV for both the initial and processed samples.

The specific surface area values exhibited a progressive increase, ranging from 24.9 to 37.4 m^2/g with a grinding time of 120 minutes. However, when subjected to prolonged mechanical treatment beyond 120 minutes, re-agglomeration occurred, resulting in a reduction in the specific surface area to 34.4 m^2/g.

The photocatalytic activity of the obtained powders was assessed through the photocatalytic oxidation of tetracycline hydrochloride. The study demonstrated that planetary milling facilitated the production of graphitic carbon nitride powder with significantly enhanced photocatalytic properties. This enhancement was evident in the threefold increase in the degradation rate constant of the antibiotic under solar light exposure.

Consequently, this investigation has underscored the viability of developing an efficacious and environmentally sustainable foundation for photocatalytic materials rooted in graphitic carbon nitride, which holds promise for the removal of hazardous organic pollutants from pharmaceutical wastewater.

References

[1] Caban M., Stepnowski P. How to Decrease Pharmaceuticals in the Environment? A Review. *Environ. Chem. Lett.*, 2021, **19**, P. 3115–3138.

[2] Abdel S.M., Gad-allah T.A., El-Shahat M.F., Ashmawy A.M., Ibrahim H.S. Novel Application of Metal-Free Graphitic Carbon Nitride (g-C_3N_4) in Photocatalytic Reduction – Recovery of Silver Ions. *J. of Environmental Chemical Engineering*, 2016, **4**, P. 4165–4172.

[3] Sammut Bartolo N., Azzopardi L.M., Serracino-Inglott A. Pharmaceuticals and the Environment. *Early Hum. Dev.*, 2021, **155**, P. 39–42.

[4] Paut Kusturica M., Jevtic M., Ristovski J.T. Minimizing the Environmental Impact of Unused Pharmaceuticals: Review Focused on Prevention. *Front. Environ. Sci.*, 2022, **10**, P. 1–8.

[5] Rapti I., Kourkouta T., Malisova E.M., Albanis T., Konstantinou I. Photocatalytic Degradation of Inherent Pharmaceutical Concentration Levels in Real Hospital WWTP Effluents Using g-C_3N_4 Catalyst on CPC Pilot Scale Reactor. *Molecules*, 2023, **28** (3), 1170.

[6] Song J., Zhao K., Yin X., Liu Y., Khan I., Wang K. Photocatalytic Degradation of Tetracycline Hydrochloride with g-C_3N_4/Ag/AgBr Composites. *Front. Chem.*, 2022, **10**, 1069816.

[7] García-López E.I., Pomilla F.R., Bloise E., Lü X., Mele G., Palmisano L., Marcì G. C_3N_4 Impregnated with Porphyrins as Heterogeneous Photocatalysts for the Selective Oxidation of 5-Hydroxymethyl-2-Furfural Under Solar Irradiation. *Top. Catal.*, 2021, **64**, P. 758–771.

[8] Rodríguez-López L., Santás-Miguel V., Cela-Dablanca R., Núnez-Delgado A., Álvarez-Rodríguez E., Pérez-Rodríguez P., Arias-Estévez M. Ciprofloxacin and Trimethoprim Adsorption/Desorption in Agricultural Soils. *Int. J. Environ. Res. Public Health*, 2022, **19** (14), 8426.

[9] Seroglazova A.S., Chebanenko M.I., Popkov V.I. Synthesis, Structure, and Photo-Fenton Activity of $PrFeO_3$–TiO_2 Mesoporous Nanocomposites. *Condens. Matter Interphases*, 2021, **23**, P. 548–560.

[10] Zhurenok A.V., Vasichenko D.B., Berdyugin S.N., Gerasimov E.Yu., Saraev A.A., Cherepanova S.V., Kozlova E.A. Photocatalysts Based on Graphite-like Carbon Nitride with a Low Content of Rhodium and Palladium for Hydrogen Production under Visible Light. *Nanomaterials*, 2023, **13**, 2176.

[11] Gupta B.K., Kedawat G., Agrawal Y., Kumar P., Dwivedi J., Dhawan S.K. A Novel Strategy to Enhance Ultraviolet Light Driven Photocatalysis from Graphene Quantum Dots Infilled TiO_2 Nanotube Arrays. *RSC Adv.*, 2015, **5**, P. 10623–10631.

[12] Chebanenko M.I., Omarov S.O., Lobinsky A.A., Nevedomskiy V.N., Popkov V.I. Steam Exfoliation of Graphitic Carbon Nitride as Efficient Route toward Metal-Free Electrode Materials for Hydrogen Production. *Int. J. Hydrogen Energy*, 2023, **48**, P. 27671–27678.

[13] Rodionov I.A., Zvereva I.A. Photocatalytic Activity of Layered Perovskite-like Oxides in Practically Valuable Chemical Reactions. *Russ. Chem. Rev.*, 2016, **85**, P. 248–279.

[14] Papailias I., Todorova N., Giannakopoulou T., Ioannidis N., Boukos N., Athanasekou C.P., Dimotikali D., Trapalis C. Chemical vs Thermal Exfoliation of g-C_3N_4 for NOx Removal under Visible Light Irradiation. *Appl. Catal. B Environ.*, 2018, **239**, P. 16–26.

[15] Xu J., Zhang L., Shi R., Zhu Y. Chemical Exfoliation of Graphitic Carbon Nitride for Efficient Heterogeneous Photocatalysis. *J. Mater. Chem. A*, 2013, **1**, P. 14766–14772.

[16] Yuan Y.J., Shen Z., Wu S., Su Y., Pei L., Ji Z., Ding M., Bai W., Chen Y., Yu Z.T. Liquid Exfoliation of g-C_3N_4 Nanosheets to Construct 2D-2D MoS2/g-C_3N_4 Photocatalyst for Enhanced Photocatalytic H_2 Production Activity. *Appl. Catal. B Environ.*, 2019, **246**, P. 120–128.

[17] Chebanenko M.I., Zakharova N.V., Popkov V.I. Synthesis and Visible-Light Photocatalytic Activity of Graphite-like Carbon Nitride Nanopowders. *Russ. J. Appl. Chem.*, 2020, **93**, P. 494–501.

[18] Chebanenko M.I., Zakharova N.V., Lobinsky A.A., Popkov V.I. Ultrasonic-Assisted Exfoliation of Graphitic Carbon Nitride and Its Electrocatalytic Performance in Process of Ethanol Reforming. *Semiconductors*, 2019, **53**, P. 2072–2077.

[19] Bokuniaeva A.O., Vorokh A.S. Estimation of Particle Size Using the Debye Equation and the Scherrer Formula for Polyphasic TiO_2 Powder. *J. Phys. Conf. Ser.*, 2019, **1410**, 012057.

[20] Qu D., Liu J., Miao X., Han M., Zhang H., Cui Z., Sun S., Kang Z., Fan H., Sun Z. Peering into Water Splitting Mechanism of g-C_3N_4-Carbon Dots Metal-Free Photocatalyst. *Appl. Catal. B Environ.*, 2018, **227**, P. 418–424.

[21] Fina F., Callear S.K., Carins G.M., Irvine J.T.S. Structural Investigation of Graphitic Carbon Nitride via XRD and Neutron Diffraction. *Chem. Mater.*, 2015, **27**, P. 2612–2618.

[22] Azizi-Toupkanloo H., Karimi-Nazarabad M., Shakeri M., Eftekhari M. Photocatalytic Mineralization of Hard-Degradable Morphine by Visible Light-Driven Ag@g-C_3N_4 Nanostructures. *Environ. Sci. Pollut. Res.*, 2019, **26**, P. 30941–30953.

[23] Zhu B., Zhang L., Cheng B., Yu J. First-Principle Calculation Study of Tri-s-Triazine-Based g-C_3N_4: A Review. *Appl. Catal. B Environ.*, 2018, **224**, P. 983–999.

Submitted 22 October 2023; revised 30 October 2023; accepted 31 October 2023

Information about the authors:

Maria I. Chebanenko – Ioffe Institute, Politechnicheskaya, 26, St. Petersburg, 194021, Russia; ORCID 0000-0002-1461-579X; m_chebanenko@list.ru

Lev A. Lebedev – Ioffe Institute, Politechnicheskaya, 26, St. Petersburg, 194021, Russia; ORCID 0000-0001-9449-9487; 1595lion@gmail.com

Maksim I. Tenevich – Ioffe Institute, Politechnicheskaya, 26, St. Petersburg, 194021, Russia; ORCID 0000-0003-2003-0672; chwm420@gmail.com

Ekaterina Yu. Stovpiaga – Ioffe Institute, Politechnicheskaya, 26, St. Petersburg, 194021, Russia; ORCID 0000-0003-0434-5252; kattrof@gvg.ioffe.ru

Vadim I. Popkov – Ioffe Institute, Politechnicheskaya, 26, St. Petersburg, 194021, Russia; ORCID 0000-0002-8450-4278; vadim.i.popkov@mail.ioffe.ru

Conflict of interest: the authors declare no conflict of interest.